Published in final edited form as:
J Perinat Med. 2014 September 1; 42(5): 549–557. doi:10.1515/jpm-2014-0073.

Effect of depth on shear-wave elastography estimated in the internal and external cervical os during pregnancy

Edgar Hernandez-Andrade[1,2], **Alma Aurioles-Garibay**[1,2], **Maynor Garcia**[1,2], **Steven J. Korzeniewski**[1,2], **Alyse G. Schwartz**[1,2], **Hyunyoung Ahn**[1,2], **Alicia Martinez-Varea**[1], **Lami Yeo**[1,2], **Tinnakorn Chaiworapongsa**[1,2], **Sonia S. Hassan**[1,2], and **Roberto Romero**[1,3,4]

[1]Perinatology Research Branch, NICHD/NIH/DHHS, Bethesda, Maryland, and Detroit, MI, USA

[2]Department of Obstetrics/Gynecology, Wayne State University School of Medicine, Detroit, MI

[3]Department of Obstetrics and Gynecology, University of Michigan, Ann Arbor, MI

[4]Department of Epidemiology and Biostatistics, Michigan State University, East Lansing, MI, USA

Abstract

Aim—To investigate the effect of depth on cervical shear-wave elastography.

Methods—Shear-wave elastography was applied to estimate the velocity of propagation of the acoustic force impulse (shear-wave) in the cervix of 154 pregnant women at 11-36 weeks of gestation. Shear-wave speed (SWS) was evaluated in cross-sectional views of the internal and external cervical os in five regions of interest: anterior, posterior, lateral right, lateral left, and endocervix. Distance from the center of the US transducer to the center of the each region of interest was registered.

Results—In all regions, SWS decreased significantly with gestational age (p=0.006). In the internal os SWS was similar among the anterior, posterior and lateral regions, and lower in the endocervix. In the external os, the endocervix and anterior regions showed similar SWS values, lower than those from the posterior and lateral regions. In the endocervix, these differences remained significant after adjustment for depth, gestational age and cervical length. SWS estimations in all regions of the internal os were higher than those of the external os, suggesting denser tissue.

Conclusion—Depth from the ultrasound probe to different regions in the cervix did not significantly affect the SWS estimations.

Keywords

cervical elasticity; cervical length; short cervix; strain; elastic Young's modulus

Address correspondence to: Roberto Romero, MD, D. Med. Sci., and Edgar Hernandez-Andrade, MD, PhD, Perinatology Research Branch, NICHD/NIH/DHHS, Wayne State University / Hutzel Women's Hospital, 3990 John R, Box 4, Detroit, Michigan, 48201 USA, Telephone: 313-993-2700, Fax: 313-993-2694, romeror@mail.nih.gov & ehernand@med.wayne.edu.

Introduction

Shear-wave elastography is considered a dynamic method to evaluate the elastic properties of tissues [1-3]. The ultrasound system produces an acoustic radiation force impulse (ARFI) [4] that creates a cone-shaped disturbance, known as shear-wave, which propagates through the tissues at high velocity, and can be tracked using superfast ultrasound with frame rates between 5000-20000 KHz [5-13]. The velocity of shear-wave propagation is estimated in meters per second and is faster in hard or stiff tissues than in soft tissues. It can also be transformed as a Young's elastic modulus and expressed in kilopascals, or displayed as a color code elastogram [8, 14, 15]. Shear-wave elastography involves three processes: 1) emission and display of the fundamental ultrasound image, 2) emission of the acoustic force impulse, and 3) estimation of shear-wave speed. The final frequency of the color elastograms on the ultrasoundscreen is about 3-5 frames per second [1].

Shear-wave elastography has been previously applied in the evaluation of the cervix in pregnant women. Gennisson et al. [16] reported a lower elastic modulus in cervix measuring <25 mm as compared with longer cervix. Carsson et al. [17] studied samples of human cervix obtained after hysterectomy and artificially induced cervical ripening before surgery with prostaglandins. They were able to demonstrate differences in shear-wave speed (SWS) when compared with unripe cervix. They also reported differences in shear-wave speed between the proximal (internal) and distal (external) portions of the cervix.

One of the advantages of shear-wave elastography over other elastography methods is that the generation of the mechanical impulse is operator-independent. Still, other factors might influence shear-wave propagation. The aim of this study was to investigate if the depth from the ultrasound transducer to the studied region can affect the shear-wave speed estimation.

Methods

Study Design & Participants

This prospective cohort study was performed at the Center for Advanced Obstetrical Care and Research [Perinatology Research Branch of the *Eunice Kennedy Shriver* National Institute of Child Health and Human Development (NICHD), National Institutes of Health, Wayne State University School of Medicine, Hutzel Women's Hospital, Detroit MI]. One hundred and fifty four (154) patients with uncomplicated singleton pregnancies were examined at 11-36 weeks of gestation. All patients provided written informed consent for ultrasound examination and were enrolled in research protocols approved by the Human Investigation Committee of Wayne State University, and the Institutional Review Board of the NICHD.

Ultrasound Examination

The cervix was evaluated using transvaginal ultrasound with an endocavitary probe 12-3 MHz (SuperSonic Imagine, Aix-en-Provence,France). Shear-wave elastography was estimated in two cross-sectional planes of the cervix, one at the level of the internal os, and the other at the level of the external os. After measurement of the cervical length [18, 19], the ultrasound probe was rotated 90° for obtain cross-sectional views. The decision to

evaluate cross-sectional images of the cervix was based on the locations of the regions of interest. The studied areas can be aligned in the center of the ultrasound beam for a regular propagation of the acoustic force impulse. We also aimed to compare areas within the same anatomic regions differing only in the distance from the ultrasound probe.

The elastogram box was adjusted to cover the entire cervix. The operator maintained a fixed position with the ultrasound probe and the patient was asked for voluntary temporal apnea. The system took approximately 3-5 seconds to show consistent color elastograms; the selected images were saved for off-line analysis. The color-coded elastogram displayed the areas with high shear-wave speed in blue, and those with slow shear-wave speed in red. Faster shear-wave propagation is related to denser or stiff tissue, and slow shear-wave propagation to soft tissue [1]. The ultrasound equipment simultaneously displayed the fundamental ultrasound image with and without the superimposed color elastogram. Shear-wave speed calculations were performed in the fundamental ultrasound image without the color elastogram using a circular region of interest (Q-box) 5 mm diameter. A total of five regions of interest were investigated in each cervical projection: one in the endocervical canal and one in each of the four quadrants of the cervix (anterior, lateral right, lateral left, and posterior) (Figures 1 and 2). All regions were aligned and equidistant from the center of the cervix. The distance in *mm* from the center of the ultrasound probe to the center of each region of interest was registered. The quantitative evaluation of shear-wave speed was expressed in meters/second *(m/s)*.

Statistical Analysis

Normality of shear-wave speed and distance from the ultrasound probe was assessed using the Kolmogorov-Smirnov test and visual inspection of histograms. Generalized linear models were fit to examine mean differences, accounting for the clustering of multiple measurements within unique patients (e.g., distance measurements performed in multiple regions of interest for a unique patient). These models included fixed effects representing the anatomical plane and measurement region, in addition to the gestational age at the time of the scan. A p value <0.05 was considered statistically significant. Statistical analyses were performed using SAS version 9.3 (Cary, N. C., USA).

Results

Characteristics of the study population are displayed in Table 1. The median gestational age at examination was 21 weeks and the median cervical length was 37 mm (IQR: 33-41). Previous preterm delivery was documented in 11.6% of patients, and 92.2% were African-American; all patients delivered at term. No differences in shear wave speed related to ethnicity or obstetrical history were documented in any of the studied regions.

Internal cervical os

Shear-wave speed estimations and distance from the ultrasound probe to each of the studied regions in the internal cervical os are presented in Table 2. Depth was significantly different between the anterior and posterior regions and from all other regions (all $p <0.0001$). No significant differences in depth between the lateral regions were documented.

Figure 3 shows the estimated mean $\log^2$ shear-wave speed for each region of interest by gestational age (continuous Figure 3A; quartile Figure 3B). The estimated shear-wave speed for measures obtained in each region of interest decreased significantly in relation to gestational age (p=0.006). Shear-wave speed in the endocervical canal was significantly lower than in all other regions of interest (p<0.01) only after 14 weeks of gestation. No significant differences in shear-wave speed were documented among anterior, posterior and lateral regions at any gestational period. Adjustment for cervical length and depth did not alter these findings (Figure 3C). The average shear-wave speed of all four regions of interest did not significantly differ from any of the individual measurements.

External cervical os

Shear-wave speed and depth from each of the studied regions of the external cervical os are presented in Table 3. Depth was also significantly different between the anterior and posterior regions and from all other regions (all p <0.001). No differences in depth between the lateral regions were noted. All regions showed lower shear-wave speed as compared to similar regions in the internal cervical os (p <0.0001 with Bonferroni adjustment).

Figure 4 shows the estimated mean $\log^2$ shear-wave speed for measures obtained in the external os. Shear-wave speed from all regions of interest decreased significantly in relation to gestational age (continuous gestational age Figure 4A; quartile gestational age Figure 4B). Shear-wave speed from the anterior region was similar to that in the endocervix and lower than in the posterior and lateral regions, and shear-wave speed from the posterior region was significantly higher than in the left lateral region. Shear-wave speed did not differ among the lateral regions but was significantly lower in the endocervix, despite being located at a similar depth. Depth did not show a significant association with shear-wave speed estimations (p=0.10). Differences in shear-wave speed of the posterior and lateral regions, when compared to the endocervical region, remained significant after adjusting for cervical length and depth (Figure 4C).

Discussion

The principal findings of this study are: 1) distance from the ultrasound transducer to different regions of interest in the cervix did not meaningfully affect shear-wave speed estimations; 2) in the internal cervical os, shear-wave speed was only lower in the endocervix as compared with all other regions. In the external cervical os, shear-wave speed was different among specific regions of interest; 3) shear-wave speed was significantly higher in all regions of the internal os as compared to those from the external os, thus suggesting denser tissue. Differences in shear-wave speed might be related to tissue characteristics rather than depth.

Clinical applications of shear-wave elastography include the evaluation of tumors [20-25], assessment of the stiffness in carotid artery plaque [26, 27], evaluation of the tensile properties of tendons and muscles [28-30], evaluation of liver disease [31-34], and assessment of deep venous thrombosis [35, 36]. In pregnant women, in addition to the preliminary reports on the cervix [16], Li et al. [37] reported a similar elastic modulus between the central and peripheral areas of the placenta. The main advantages of shear-wave

elastography using acoustic force impulse are: 1) the creation of the tissue disturbance is operator-independent, 2) it provides a quantitative evaluation of the propagation of the shear-wave, and 3) the stimulus travels longer distances.

Depth and shear-wave speed

The influence of depth in shear-wave speed was previously evaluated by Chang et al. [38] in a phantom model. The authors reported an averaged reduction in shear-wave speed of 0.1 m/s per centimeter of increased depth. These differences became significant when the structure was located at ≥3 cm from the transducer [38]. Transvaginal ultrasound may reduce the attenuation effect of depth on shear-wave elastography as none of the studied regions were located deeper than 3 cm. In the external os, all regions of interest were located even closer to the ultrasound probe than those from the internal os; therefore, a lower impact of depth on shear wave signals might be expected. Nonetheless, shear-wave speed was higher in the posterior than the anterior regions. This difference in shear-wave propagation might be related to differences in tissue constitution as values remained significant after adjustment by depth. The velocity of propagation of the shear-wave can be related to the alignment and organization of the collagen network, concentration of proteoglycans [39] [40-44], and the amount of smooth muscle cells [45, 46] [47] in different cervical regions.

Elastography and the cervix

Ultrasound elastography has been previously applied to investigate the elastic properties of the cervix [48-51]. The first studies were based on the qualitative evaluation of color elastograms [52, 53]. Recent reports proposed standard protocols for image acquisition and analysis, providing numerical values, thus improving the reliability of the method [48, 49, 54, 55]. Our group, using quasi-static elastography, reported lower strain values in the internal cervical os than in the external cervical os [56, 57]. However, despite using a method to standardize the oscillatory compression applied by the operator, a reasonable concern arises if these differences can, at least in part, be related to the operator technique, and/or depth [58]. Shear-wave elastography generates a mechanical impulse (independent of the operator) which can be used to evaluate the effect of depth on shear-wave propagation. The results of the present study suggest that depth does not significantly affect the shear-wave propagation in the pregnant cervix. The differences observed between the internal and external os, and within regions of interest, are in agreement with those reported by Carlson et al. [17], who estimated the shear-wave speed in cervix samples obtained after hysterectomy: these authors showed differences in the propagation of the shear-wave along the length of the cervix, with the highest speed obtained in the proximal portion (internal os), and with a constant reduction towards the distal portion (external os). They also reported differences between the anterior and posterior segments of the external cervical os. Accordingly, the internal cervical os seems to be a denser area than the external os [59].

Technical comments

Previous reports on cervical elastography have been performed in a sagittal projection, similar to that used for cervical length measurement [49, 50, 52]. This is a practical approach, as the operator does not modify the orientation of the ultrasound probe. The main limitation is that regions with different elastic properties are combined in the final

calculation. Cross-sectional projections of the cervix display areas with similar anatomic location and function. Our results show similar shear-wave speed estimations in different regions of the internal os, making this anatomical region more reliable for cervical evaluation. The lack of homogeneity in the external os makes the analysis of cervical elasticity challenging for elastography methods; however, other techniques might be applicable [60-67].

For adequate recordings, three sources of movement should be controlled [68]: 1) the operator must keep the US probe fixed in the same position; 2) the mother should briefly hold her breath, and 3) images must be obtained in the absence of fetal movement. The system needs approximately 3-5 seconds to display consistent color elastograms. We propose using the color elastogram to select the optimal images for shear-wave speed calculation and the gray scale ultrasound image for delineation of the region of interest.

Conclusion

Elastography techniques are promising methods to evaluate the tensile properties of the cervix during pregnancy; however, specific protocols for high quality acquisition, and training of the operators, should be implemented before clinical application. The evaluation of cervical elasticity in addition to cervical length, might improve the identification of women at risk of preterm delivery [69-75], provide information on cervical changes after progesterone treatment [76-81], and on cervical changes before the onset of labor [82-85]. The advantage of cervical elastography is that it can be evaluated during the same ultrasound scan for cervical length measurement and results might be clinically useful. The complementary information that quasi-static and shear-wave elastography can provide on cervical characteristics during pregnancy should be further evaluated.

Summary

Depth did not meaningfully affect the estimation of shear-wave speed in the cervix of pregnant women. Differences in shear-wave speed among cervical regions os might be related to tissue constitution.

Acknowledgments

This research was supported, in part, by the Perinatology Research Branch, Division of Intramural Research, *Eunice Kennedy Shriver* National Institute of Child Health and Human Development, National Institutes of Health, Department of Health and Human Services (NICHD/NIH); and, in part, with Federal funds from NICHD, NIH under Contract No. HHSN275201300006C. The ultrasound experience and technical support of senior Registered Diagnostic Medical Sonographers (RDMS), Mrs. Catherine Ducharme, Mrs. Denise Haggerty and Cara Staszewski are gratefully acknowledged.

References

1. Bamber J, Cosgrove D, Dietrich CF, Fromageau J, Bojunga J, Calliada F, et al. EFSUMB guidelines and recommendations on the clinical use of ultrasound elastography. Part 1: Basic principles and technology. Ultraschall Med. 2013; 34:169–84. [PubMed: 23558397]
2. Garra BS. Imaging and estimation of tissue elasticity by ultrasound. Ultrasound Q. 2007; 23:255–68. [PubMed: 18090836]
3. Parker KJ, Doyley MM, Rubens DJ. Imaging the elastic properties of tissue: the 20 year perspective. Phys Med Biol. 2011; 56:R1–R29. [PubMed: 21119234]

4. Torr GR. The acoustic radiation force. Am J Phys. 1984; 52:402–8.
5. Nightingale K. Acoustic Radiation Force Impulse (ARFI) Imaging: a Review. Curr Med Imaging Rev. 2011; 7:328–39. [PubMed: 22545033]
6. Muthupillai R, Lomas DJ, Rossman PJ, Greenleaf JF, Manduca A, Ehman RL. Magnetic resonance elastography by direct visualization of propagating acoustic strain waves. Science. 1995; 269:1854–7. [PubMed: 7569924]
7. Nightingale KR, Palmeri ML, Nightingale RW, Trahey GE. On the feasibility of remote palpation using acoustic radiation force. J Acoust Soc Am. 2001; 110:625–34. [PubMed: 11508987]
8. Palmeri ML, Nightingale KR. Acoustic radiation force-based elasticity imaging methods. Interface Focus. 2011; 1:553–64. [PubMed: 22419986]
9. Nightingale K, Soo MS, Nightingale R, Trahey G. Acoustic radiation force impulse imaging: in vivo demonstration of clinical feasibility. Ultrasound Med Biol. 2002; 28:227–35. [PubMed: 11937286]
10. Nightingale K, McAleavey S, Trahey G. Shear-wave generation using acoustic radiation force: in vivo and ex vivo results. Ultrasound Med Biol. 2003; 29:1715–23. [PubMed: 14698339]
11. Sugimoto TUS, U S, Itoh K. Tissue hardness measurement using radiation force of focused ultrasound. Proc IEEE Ultrasoun Symp NY. 1990; 3:1377–80.
12. Bercoff J, Tanter M, Fink M. Supersonic shear imaging: a new technique for soft tissue elasticity mapping. IEEE Trans Ultrason Ferroelectr Freq Control. 2004; 51:396–409. [PubMed: 15139541]
13. Nightingale KR, Z L, Dahl JJ, Frinkley KD, Palmeri ML. Shear wave velocity estimation using acoustic radiation force impulsive excitation in liver in vivo. Proc IEEE Ultrasonics Symposium Vanc. 2006:1156–60.
14. Sarvazyan AP, Rudenko OV, Swanson SD, Fowlkes JB, Emelianov SY. Shear wave elasticity imaging: a new ultrasonic technology of medical diagnostics. Ultrasound Med Biol. 1998; 24:1419–35. [PubMed: 10385964]
15. Palmeri ML, Wang MH, Dahl JJ, Frinkley KD, Nightingale KR. Quantifying hepatic shear modulus in vivo using acoustic radiation force. Ultrasound Med Biol. 2008; 34:546–58. [PubMed: 18222031]
16. Gennisson JL, M M, Ami O, Kohl V, Gabor P, Musset D, Tanter M. Shear wave elastography in obstetrics: Quantification of cervix elasticity and uterine contraction. Ultrasonics Symposium IEEE International. 2011:2094–7.
17. Carlson LC, Feltovich H, Palmeri ML, Dahl JJ, Munoz Del Rio A, Hall TJ. Shear wave speed estimation in the human uterine cervix. Ultrasound Obstet Gynecol. 2014; 43:452–8. [PubMed: 23836486]
18. Romero R, Yeo L, Miranda J, Hassan SS, Conde-Agudelo A, Chaiworapongsa T. A blueprint for the prevention of preterm birth: vaginal progesterone in women with a short cervix. J Perinat Med. 2013; 41:27–44. [PubMed: 23314512]
19. Burger M, Weber-Rossler T, Willmann M. Measurement of the pregnant cervix by transvaginal sonography: an interobserver study and new standards to improve the interobserver variability. Ultrasound Obstet Gynecol. 1997; 9:188–93. [PubMed: 9165682]
20. Berg WA, Cosgrove DO, Dore CJ, Schafer FK, Svensson WE, Hooley RJ, et al. Shear-wave elastography improves the specificity of breast US: the BE1 multinational study of 939 masses. Radiology. 2012; 262:435–49. [PubMed: 22282182]
21. Bojunga J, Dauth N, Berner C, Meyer G, Holzer K, Voelkl L, et al. Acoustic radiation force impulse imaging for differentiation of thyroid nodules. PLoS One. 2012; 7:e42735. [PubMed: 22952609]
22. Cosgrove DO, Berg WA, Dore CJ, Skyba DM, Henry JP, Gay J, et al. Shear wave elastography for breast masses is highly reproducible. Eur Radiol. 2012; 22:1023–32. [PubMed: 22210408]
23. Evans A, Whelehan P, Thomson K, McLean D, Brauer K, Purdie C, et al. Quantitative shear wave ultrasound elastography: initial experience in solid breast masses. Breast Cancer Res. 2010; 12:R104. [PubMed: 21122101]
24. Ahmad S, Cao R, Varghese T, Bidaut L, Nabi G. Transrectal quantitative shear wave elastography in the detection and characterisation of prostate cancer. Surg Endosc. 2013; 27:3280–7. [PubMed: 23525883]

25. Chang JM, Park IA, Lee SH, Kim WH, Bae MS, Koo HR, et al. Stiffness of tumours measured by shear-wave elastography correlated with subtypes of breast cancer. Eur Radiol. 2013; 23:2450–8. [PubMed: 23673574]
26. Ramnarine KV, Garrard JW, Dexter K, Nduwayo S, Panerai RB, Robinson TG. Shear Wave Elastography Assessment of Carotid Plaque Stiffness: In Vitro Reproducibility Study. Ultrasound Med Biol. 2013
27. Garrard JW, Ramnarine KV. Shear-Wave Elastography in Carotid Plaques: Comparison with Grayscale Median and Histological Assessment in an Interesting Case. Ultraschall Med. 2013
28. Eby SF, Song P, Chen S, Chen Q, Greenleaf JF, An KN. Validation of shear wave elastography in skeletal muscle. J Biomech. 2013; 46:2381–7. [PubMed: 23953670]
29. Ooi CC, Malliaras P, Schneider ME, Connell DA. "Soft, hard, or just right?" Applications and limitations of axial-strain sonoelastography and shear-wave elastography in the assessment of tendon injuries. Skeletal Radiol. 2014; 43:1–12. [PubMed: 23925561]
30. Aubry S, Risson JR, Kastler A, Barbier-Brion B, Siliman G, Runge M, et al. Biomechanical properties of the calcaneal tendon in vivo assessed by transient shear wave elastography. Skeletal Radiol. 2013; 42:1143–50. [PubMed: 23708047]
31. Friedrich-Rust M, Wunder K, Kriener S, Sotoudeh F, Richter S, Bojunga J, et al. Liver fibrosis in viral hepatitis: noninvasive assessment with acoustic radiation force impulse imaging versus transient elastography. Radiology. 2009; 252:595–604. [PubMed: 19703889]
32. Kircheis G, Sagir A, Vogt C, Vom Dahl S, Kubitz R, Haussinger D. Evaluation of acoustic radiation force impulse imaging for determination of liver stiffness using transient elastography as a reference. World J Gastroenterol. 2012; 18:1077–84. [PubMed: 22416182]
33. Lupsor M, Badea R, Stefanescu H, Sparchez Z, Branda H, Serban A, et al. Performance of a new elastographic method (ARFI technology) compared to unidimensional transient elastography in the noninvasive assessment of chronic hepatitis C. Preliminary results. J Gastrointestin Liver Dis. 2009; 18:303–10. [PubMed: 19795024]
34. Yoon JH, Lee JY, Woo HS, Yu MH, Lee ES, Joo I, et al. Shear wave elastography in the evaluation of rejection or recurrent hepatitis after liver transplantation. Eur Radiol. 2013; 23:1729–37. [PubMed: 23300037]
35. Bernal M, Gennisson JL, Flaud P, Tanter M. Shear wave elastography quantification of blood elasticity during clotting. Ultrasound Med Biol. 2012; 38:2218–28. [PubMed: 23069137]
36. Huang CC, Chen PY, Shih CC. Estimating the viscoelastic modulus of a thrombus using an ultrasonic shear-wave approach. Med Phys. 2013; 40:042901. [PubMed: 23556923]
37. Li WJ, Wei ZT, Yan RL, Zhang YL. Detection of placenta elasticity modulus by quantitative real-time shear wave imaging. Clin Exp Obstet Gynecol. 2012; 39:470–3. [PubMed: 23444746]
38. Chang S, Kim MJ, Kim J, Lee MJ. Variability of shear wave velocity using different frequencies in acoustic radiation force impulse (ARFI) elastography: a phantom and normal liver study. Ultraschall Med. 2013; 34:260–5. [PubMed: 23023455]
39. House M, Feltovich H, Hall TJ, Stack T, Patel A, Socrate S. Three-dimensional, extended field-of-view ultrasound method for estimating large strain mechanical properties of the cervix during pregnancy. Ultrason Imaging. 2012; 34:1–14. [PubMed: 22655487]
40. Uldbjerg N, Ekman G, Malmstrom A, Olsson K, Ulmsten U. Ripening of the human uterine cervix related to changes in collagen, glycosaminoglycans, and collagenolytic activity. Am J Obstet Gynecol. 1983; 147:662–6. [PubMed: 6638110]
41. Osmers R, Rath W, Pflanz MA, Kuhn W, Stuhlsatz HW, Szeverenyi M. Glycosaminoglycans in cervical connective tissue during pregnancy and parturition. Obstet Gynecol. 1993; 81:88–92. [PubMed: 8416467]
42. Fittkow CT, Shi SQ, Bytautiene E, Olson G, Saade GR, Garfield RE. Changes in light-induced fluorescence of cervical collagen in guinea pigs during gestation and after sodium nitroprusside treatment. J Perinat Med. 2001; 29:535–43. [PubMed: 11776685]
43. Shi L, Shi SQ, Saade GR, Chwalisz K, Garfield RE. Changes in cervical resistance and collagen fluorescence during gestation in rats. J Perinat Med. 1999; 27:188–94. [PubMed: 10503180]
44. Winkler M, Rath W. Changes in the cervical extracellular matrix during pregnancy and parturition. J Perinat Med. 1999; 27:45–60. [PubMed: 10343934]

45. Kling E, Kitahara S, Posligua L, Malpica A, Silva EG. The 2 stromal compartments of the normal cervix with distinct immunophenotypic and histomorphologic features. Ann Diagn Pathol. 2012; 16:315–22. [PubMed: 22503284]
46. deSouza NM, Hawley IC, Schwieso JE, Gilderdale DJ, Soutter WP. The uterine cervix on in vitro and in vivo MR images: a study of zonal anatomy and vascularity using an enveloping cervical coil. AJR. 1994; 163:607–12. [PubMed: 8079853]
47. Ross, M.; Wojciech, P. Female Reproductive System. In: Ross, Michael H.; Pawlina, Wojciech, editors. Histology A Text and Atlas. 6. Lippincott Williams & Wilkins; USA: 2010. p. 830-92.
48. Fruscalzo A, Schmitz R. Quantitative cervical elastography in pregnancy. Ultrasound Obstet Gynecol. 2012; 40:612. [PubMed: 23168975]
49. Molina F, Gomez L, Florido J, Padilla M, Nicolaides K. Quantification of cervical elastography. A reproducibility study. Ultrasound Obstet Gynecol. 2012; 39:685–9. [PubMed: 22173854]
50. Fruscalzo A, Steinhard J, Londero AP, Frohlich C, Bijnens B, Klockenbusch W, et al. Reliability of quantitative elastography of the uterine cervix in at-term pregnancies. J Perinat Med. 2013:1–7.
51. Khalil MR, Thorsen P, Uldbjerg N. Cervical ultrasound elastography may hold potential to predict risk of preterm birth. Dan Med J. 2013; 60:A4570. [PubMed: 23340191]
52. Swiatkowska-Freund M, Preis K. Elastography of the uterine cervix: implications for success of induction of labor. Ultrasound Obstet Gynecol. 2011; 38:52–6. [PubMed: 21484905]
53. Thomas A. Imaging of the cervix using sonoelastography. Ultrasound Obstet Gynecol. 2006; 28:356–7. [PubMed: 16909409]
54. Hwang HS, Sohn IS, Kwon HS. Imaging analysis of cervical elastography for prediction of successful induction of labor at term. J Ultrasound Med. 2013; 32:937–46. [PubMed: 23716514]
55. Thomas A, Kummel S, Gemeinhardt O, Fischer T. Real-time sonoelastography of the cervix: tissue elasticity of the normal and abnormal cervix. Acad Radiol. 2007; 14:193–200. [PubMed: 17236992]
56. Hernandez-Andrade E, Hassan SS, Ahn H, Korzeniewski SJ, Yeo L, Chaiworapongsa T, et al. Evaluation of cervical stiffness during pregnancy using semiquantitative ultrasound elastography. Ultrasound Obstet Gynecol. 2013; 41:152–61. [PubMed: 23151941]
57. Hernandez-Andrade E, Romero R, Korzeniewski SJ, Ahn H, Aurioles-Garibay A, Garcia M, et al. Cervical strain determined by ultrasound elastography and its association with spontaneous preterm delivery. J Perinat Med. 2013:1–11.
58. Mazza E, Parra-Saavedra M, Bajka M, Gratacos E, Nicolaides K, Deprest J. In-vivo assessment of the biomechanical properties of the uterine cervix in pregnancy. Prenat Diagn. 2013
59. Wells PN, Liang HD. Medical ultrasound: imaging of soft tissue strain and elasticity. J R Soc Interface. 2011; 8:1521–49. [PubMed: 21680780]
60. Mazza E, Nava A, Bauer M, Winter R, Bajka M, Holzapfel GA. Mechanical properties of the human uterine cervix: an in vivo study. Med Image Anal. 2006; 10:125–36. [PubMed: 16143559]
61. Maul H, Olson G, Fittkow CT, Saade GR, Garfield RE. Cervical light-induced fluorescence in humans decreases throughout gestation and before delivery: Preliminary observations. Am J Obstet Gynecol. 2003; 188:537–41. [PubMed: 12592268]
62. McFarlin BL, Bigelow TA, Laybed Y, O'Brien WD, Oelze ML, Abramowicz JS. Ultrasonic attenuation estimation of the pregnant cervix: a preliminary report. Ultrasound Obstet Gynecol. 2010; 36:218–25. [PubMed: 20629011]
63. Feltovich H, Nam K, Hall TJ. Quantitative ultrasound assessment of cervical microstructure. Ultrason Imaging. 2010; 32:131–42. [PubMed: 20718243]
64. Yilmaz NC, Yigiter AB, Kavak ZN, Durukan B, Gokaslan H. Longitudinal examination of cervical volume and vascularization changes during the antepartum and postpartum period using three-dimensional and power Doppler ultrasound. J Perinat Med. 2010; 38:461–5. [PubMed: 20629490]
65. Kuwata T, Matsubara S, Taniguchi N, Ohkuchi A, Ohkusa T, Suzuki M. A novel method for evaluating uterine cervical consistency using vaginal ultrasound gray-level histogram. J Perinat Med. 2010; 38:491–4. [PubMed: 20443760]
66. Tekesin I, Wallwiener D, Schmidt S. The value of quantitative ultrasound tissue characterization of the cervix and rapid fetal fibronectin in predicting preterm delivery. J Perinat Med. 2005; 33:383–91. [PubMed: 16238532]

67. Garfield RE, Chwalisz K, Shi L, Olson G, Saade GR. Instrumentation for the diagnosis of term and preterm labour. J Perinat Med. 1998; 26:413–36. [PubMed: 10224598]
68. Fahey BJ, Palmeri ML, Trahey GE. The impact of physiological motion on tissue tracking during radiation force imaging. Ultrasound Med Biol. 2007; 33:1149–66. [PubMed: 17451869]
69. Hassan SS, Romero R, Berry SM, Dang K, Blackwell SC, Treadwell MC, et al. Patients with an ultrasonographic cervical length < or =15 mm have nearly a 50% risk of early spontaneous preterm delivery. Am J Obstet Gynecol. 2000; 182:1458–67. [PubMed: 10871466]
70. Hassan S, Romero R, Hendler I, Gomez R, Khalek N, Espinoza J, et al. A sonographic short cervix as the only clinical manifestation of intra-amniotic infection. J Perinat Med. 2006; 34:13–9. [PubMed: 16489881]
71. Vaisbuch E, Romero R, Erez O, Kusanovic JP, Mazaki-Tovi S, Gotsch F, et al. Clinical significance of early (< 20 weeks) vs. late (20-24 weeks) detection of sonographic short cervix in asymptomatic women in the mid-trimester. Ultrasound Obstet Gynecol. 2010; 36:471–81. [PubMed: 20503224]
72. Romero R. Prevention of spontaneous preterm birth: the role of sonographic cervical length in identifying patients who may benefit from progesterone treatment. Ultrasound Obstet Gynecol. 2007; 30:675–86. [PubMed: 17899585]
73. Heath VC, Southall TR, Souka AP, Elisseou A, Nicolaides KH. Cervical length at 23 weeks of gestation: prediction of spontaneous preterm delivery. Ultrasound Obstet Gynecol. 1998; 12:312–7. [PubMed: 9819868]
74. Iams JD, Goldenberg RL, Meis PJ, Mercer BM, Moawad A, Das A, et al. The length of the cervix and the risk of spontaneous premature delivery. National Institute of Child Health and Human Development Maternal Fetal Medicine Unit Network. N Engl J Med. 1996; 334:567–72. [PubMed: 8569824]
75. Andersen HF, Nugent CE, Wanty SD, Hayashi RH. Prediction of risk for preterm delivery by ultrasonographic measurement of cervical length. Am J Obstet Gynecol. 1990; 163:859–67. [PubMed: 2206073]
76. Hassan SS, Romero R, Vidyadhari D, Fusey S, Baxter JK, Khandelwal M, et al. Vaginal progesterone reduces the rate of preterm birth in women with a sonographic short cervix: a multicenter, randomized, double-blind, placebo-controlled trial. Ultrasound Obstet Gynecol. 2011; 38:18–31. [PubMed: 21472815]
77. Romero R, Nicolaides K, Conde-Agudelo A, Tabor A, O'Brien JM, Cetingoz E, et al. Vaginal progesterone in women with an asymptomatic sonographic short cervix in the midtrimester decreases preterm delivery and neonatal morbidity: a systematic review and metaanalysis of individual patient data. Am J Obstet Gynecol. 2012; 206:124 e1–19. [PubMed: 22284156]
78. Conde-Agudelo A, Romero R, Nicolaides K, Chaiworapongsa T, O'Brien JM, Cetingoz E, et al. Vaginal progesterone vs. cervical cerclage for the prevention of preterm birth in women with a sonographic short cervix, previous preterm birth, and singleton gestation: a systematic review and indirect comparison metaanalysis. Am J Obstet Gynecol. 2013; 208:42 e1–e18. [PubMed: 23157855]
79. Fonseca EB, Celik E, Parra M, Singh M, Nicolaides KH. Progesterone and the risk of preterm birth among women with a short cervix. N Engl J Med. 2007; 357:462–9. [PubMed: 17671254]
80. Berghella V. Novel developments on cervical length screening and progesterone for preventing preterm birth. BJOG. 2009; 116:182–7. [PubMed: 19076950]
81. Campbell S. Universal cervical-length screening and vaginal progesterone prevents early preterm births, reduces neonatal morbidity and is cost saving: doing nothing is no longer an option. Ultrasound Obstet Gynecol. 2011; 38:1–9. [PubMed: 21713990]
82. Hassan SS, Romero R, Haddad R, Hendler I, Khalek N, Tromp G, et al. The transcriptome of the uterine cervix before and after spontaneous term parturition. Am J Obstet Gynecol. 2006; 195:778–86. [PubMed: 16949412]
83. Hassan SS, Romero R, Tarca AL, Nhan-Chang CL, Mittal P, Vaisbuch E, et al. The molecular basis for sonographic cervical shortening at term: identification of differentially expressed genes and the epithelial-mesenchymal transition as a function of cervical length. Am J Obstet Gynecol. 2010; 203:472 e1–e14. [PubMed: 20817141]

84. Gonzalez JM, Dong Z, Romero R, Girardi G. Cervical remodeling/ripening at term and preterm delivery: the same mechanism initiated by different mediators and different effector cells. PloS one. 2011; 6:e26877. [PubMed: 22073213]

85. Gonzalez JM, Romero R, Girardi G. Comparison of the mechanisms responsible for cervical remodeling in preterm and term labor. J Reprod Immunol. 2013; 97:112–9. [PubMed: 23312455]

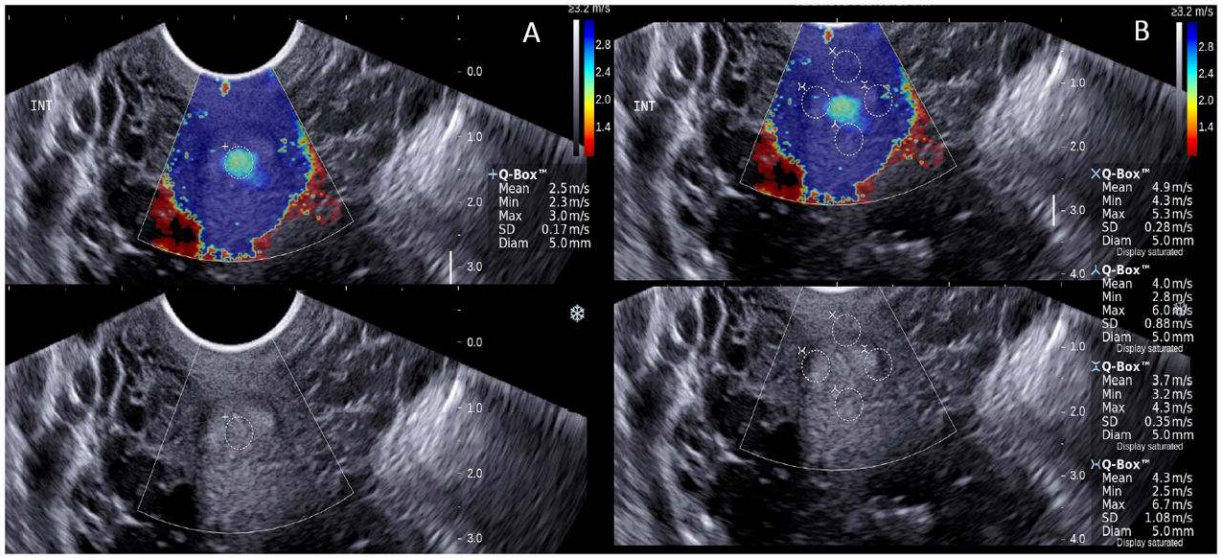

Figure 1.

Shear-wave elastography of the cross sectional view of the internal os: **1A** endocervix, **1B** anterior, posterior and lateral regions. Upper panels show the color elastogram over imposed to the fundamental ultrasound image. The color bar shows the shear-wave speed in relation to the color code. Fast shear-wave propagation is represented in blue, and can be related to denser tissue. The regions of interest (Qbox) have similar size and are located equidistant from the midline. The system allows only four simultaneous measurements, the endocervix is evaluated separately. Propagation of the shear-wave is expressed in meters per second.

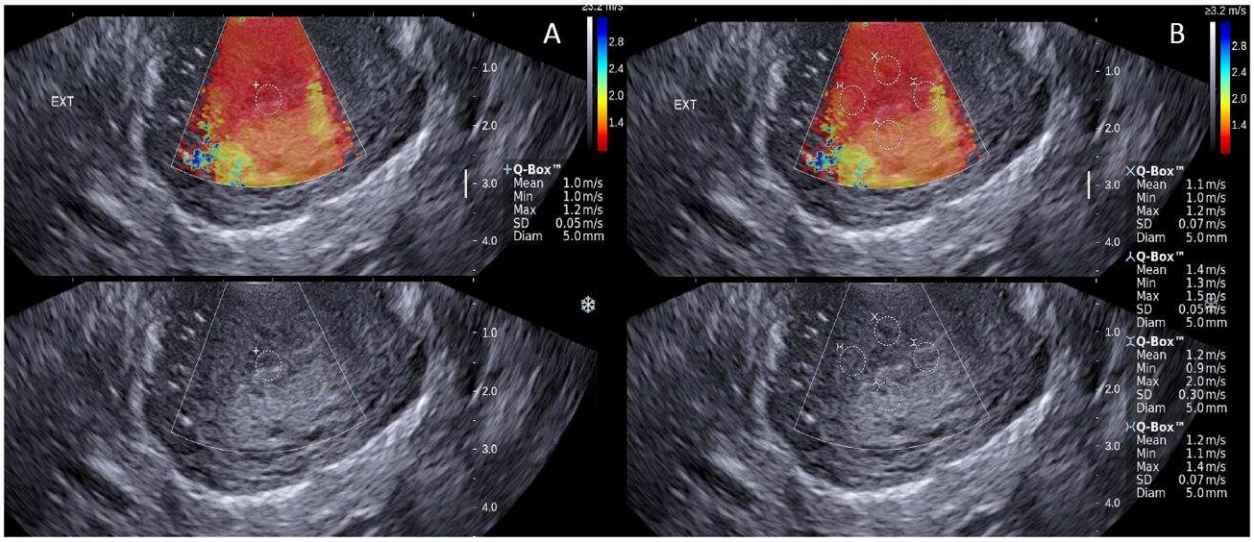

Figure 2.

Shear-wave elastography of the cross sectional view of the external os: **2A** endocervix, **2B** anterior posterior and lateral regions. Upper panels show the color elastogram over imposed to the fundamental ultrasound image. The color bar shows the shear-wave speed in relation to the color code. Slow shear-wave propagation is represented in red, and can be related to soft tissue. The regions of interest (Qbox) have similar size and are located equidistant from the midline. The system allows only four simultaneous measurements, the endocervix is evaluated separately. Propagation of the shear-wave is expressed in meters per second.

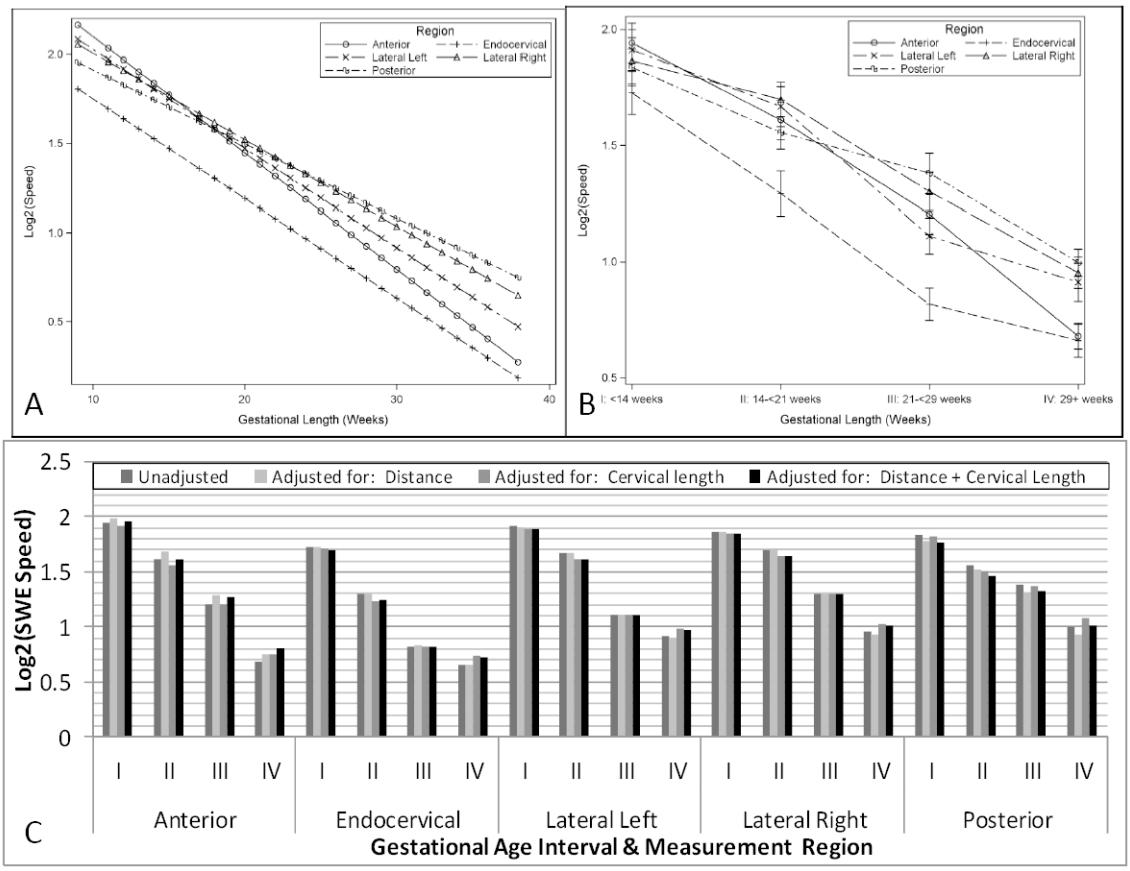

Figure 3.

Estimated mean log^2 shear-wave speed of each region of interest of the internal cervical os by continuous **(3A)**, and categorical gestational age **(3B)**. Figure **3C:** adjustment for depth and cervical length for each region of the internal os in each of the gestational periods: I, <14 weeks; II, 14-<21 weeks; III, 21-<29 weeks; IV, 29 or more weeks.

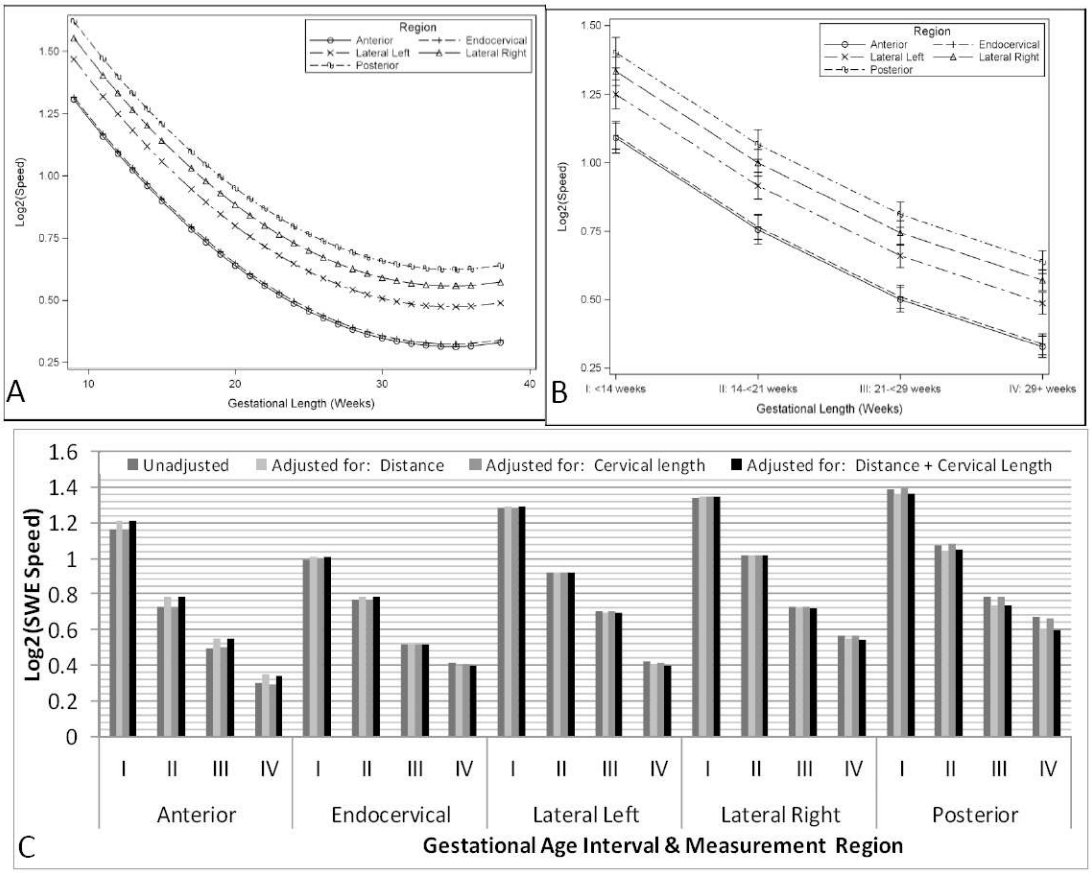

Figure 4.

Estimated mean $\log^2$ shear-wave speed of each region of interest of the external cervical os by continuous **(4A)**, and categorical gestational age **(4B)**. Figure **4C**: adjustment for depth and cervical length for each region of the internal os in each of the gestational periods: I, <14 weeks; II, 14-<21 weeks; III, 21-<29 weeks; IV, 29 or more weeks.

Table 1

Descriptive Characteristics of the study group

Characteristic	**N=154**	
	n	% or IQR
African-American	142	92.2
Maternal age (years, median)	24	21-27
Gestational age at examination (weeks median)	21	14-29
Gestational age at birth (weeks median)	39	37-40
Cervical length (mm, median)	37	33-41
Smoking	19	12.3
Nulliparous	32	20.7
Prior preterm delivery	18	11.6

IQR, interquartile range

Table 2

Distribution of shear-wave speed (m/s) and depth (mm) by region of interest in the internal cervical os

Region		Shear-wave speed (m/s)			Depth (mm)		
	N	Median	Lower Quartile	Upper Quartile	Median	Lower Quartile	Upper Quartile
Endocervix	154	2[†]	1.5	2.9	16.4	15.0	18.8
Anterior	154	2.3	1.8	3.7	10.4[*]	8.7	12.3
Posterior	148	2.6	2	3.6	21.9[*]	20.4	24.4
Lateral Right	154	2.8	1.9	3.7	17.1	15.4	19.0
Lateral Left	153	2.7	1.9	3.6	17.1	15.3	18.9

[†] Significantly different from all other regions (<0.001);

[*] significantly different among them, and from all other regions

Table 3

Distribution of shear-wave speed (m/s) and depth (mm) by region of interest in the external cervical os

Region		Shear-wave speed (m/s)			Depth (mm)		
	n	Median	Lower Quartile	Upper Quartile	Median	Lower Quartile	Upper Quartile
Endocervix	154	1.5	1.3	2	13.95	11.7	15.7
Anterior	154	1.4†	1.3	1.9	8.05*	6.4	9.7
Posterior	154	1.8	1.5	2.3	19.45*	17.0	22.1
Lateral Right	154	1.8	1.5	2.2	14.65	13.0	17.1
Lateral Left	154	1.6	1.4	2.2	14.65	13.1	16.1

† similar to the endocervical region, and significantly different from all other regions (<0.001);

* significantly different among them, and from all other regions